Three-Phase Synchrophasor Estimation Through Taylor Extended Kalman Filter

Roberto Ferrero*, Paolo Attilio Pegoraro†, Sergio Toscani‡
*Department of Electrical Engineering and Electronics, University of Liverpool, Liverpool, UK
†Department of Electrical and Electronic Engineering, University of Cagliari, Cagliari, Italy
‡Dipartimento di Elettronica, Informazione e Bioingegneria, Politecnico di Milano, Milan, Italy
email: sergio.toscani@polimi.it

***Abstract*—Synchronized phasor and frequency measurements are key tools for the monitoring and management of modern power systems. In a dynamic scenario, it is fundamental to define algorithms that allow accurately measuring time-varying signals, with short latencies and high reporting rates. A dynamic phasor model can help the design of these algorithms and, in particular, of those based on Kalman filtering approach.**

In this paper, an Extended Kalman filter formulation that considers the Taylor expansions of amplitudes and phase angles in three-phase signals is introduced. The proposed dynamic model takes into account the inherent relationship among the phases and includes harmonics in a effective way. The performance of the method permitting both synchrophasor and frequency measurements are assessed by simulations, considering also the combined effect of dynamics and disturbances. The algorithm shows tracking capabilities and the flexibility which is mandatory to deal with different conditions.

***Index Terms*—Phasor Measurement Unit, Synchrophasor estimation, Frequency, Kalman Filter, Harmonics, Three-phase systems.**

I. Introduction

Synchronized measurement of electrical signal parameters, namely amplitude, phase angle, frequency and rate of change of frequency (ROCOF), in power networks applications is a very important topic since Phasor Measurement Units (PMUs) were introduced. PMUs rely on an universal time coordinated (UTC) reference to accurately define the measurement instant and associate a timestamp with each measured quantity [1] (hence the name synchophasor). PMUs and the typical reporting rates were originally designed to deal with the usual dynamics of transmission networks; however PMUs are expected to play a significat role also in the wide area monitoring of distribution systems.

Time-varying parameters can be measured accurately only if specifically designed measurement algorithms are implemented. The combination of rapidly evolving signals and UTC-referenced timebase have led to the need for PMU algorithms that consider dynamic conditions from a very initial design stage and basically rely on dynamic estimation models.

The relevance of dynamic conditions is highlighted by the synchrophasor standards IEEE C37.118 and its evolutions IEEE C37.118.1-2011 [2] and IEEE C37.118.1a-2014 [3] (superseded by the new joint IEC-IEEE standard 60255-118-1 [4]), which introduced the definition of dynamic synchrophasor, and prescribed also dynamic tests, like amplitude and phase modulation or frequency ramp, in order to verify compliance of commercial PMUs.

For these reasons, literature on dynamic synchrophasors, frequency and ROCOF measurements is growing in recent years and different techniques have been applied. In [5], a dynamic phasor model (Taylor-Fourier, TF, model) based on a Taylor expansion of the phasor around the measurement instant is introduced. In [6], [7] discrete fourier transform (DFT) corrections based on the same model are considered. IpDFT has also been successfully applied to follow frequency variation in the presence of disturbances [8] and extended to keep into account the Taylor model [9]. In [10] the model in [5] is considered to design a two-channel PMU algorithm that can simultaneously comply with standard requirements for both protection and measurement applications, by fast reacting to fast changes in the input signal. In [11] the Taylor expansion of magnitude and phase of the Space Vector (SV) signal is used to estimate the positive sequence synchrophasor and frequency in three-phase systems, while in [12] the SV is exploited jointly with the TF model. In [13], the dynamic model is adaptively updated to include other frequency components and improve the synchrophasor estimation via compressive sensing.

The Kalman filter is often used to perform DFT-like filtering [14], but it can be extended to include the TF paradigm [15] and design a Taylor-Kalman filter (TKF) for dynamic synchrophasor tracking. In [16] the TKF is modified to improve the model of the phasor derivatives and of phase angle dynamics. In [17] a smoothed TKF with enhanced frequency estimation under off-nominal conditions is presented.

In the above formulations, the fundamental frequency component is considered. However, harmonics can be harmful for dynamic phasor estimation and directly affect TKF-based measurements. For these reasons, [18] proposes to include harmonics in the state model and in [19] the modified TKF is extended and improved to estimate both fundamental and harmonic synchrophasors under dynamic conditions.

All of these algorithms use a linear formulation of the TKF based on the Taylor expansion of the phasors, thus introducing the complex derivatives that blend together both amplitude and phase angle dynamics. In [20], a Taylor Extended Kalman filter (TEKF) is introduced, which separates the amplitude and phase angle Taylor expansions. Different expansion orders can thus be applied to amplitude and phase, while harmonics can

be tied to the fundamental component.

The characteristics of the three-phase signals have been exploited in the literature to improve synchrophasor estimation (see [21] for a SV-based approach). In this paper, TEKF is extended and improved to take advantage of the peculiarities of three-phase signals. A single model is used to include the three-phase parameters of the fundamental and harmonic components and the dynamic model keeps into account the mutual phase relationships. In particular, the frequency is seen as a common parameter of the system, reflecting the physical properties of three-phase systems. The newly proposed TEKF (3ph-TEKF) allows estimating both single-phase and positive sequence synchrophasors together with frequency. Performance is assessed by simulations of complex conditions that combine different test signals from [2], [4], [22] also including three-phase unbalance [23] in order to stress dynamic tracking and disturbance rejection capabilities of the algorithm.

II. Three-Phase Taylor Extended Kalman Filter Synchrophasor Estimator

The implementation of a Kalman filter-based algorithm allowing synchrophasor and frequency estimation from measurement data basically requires that three relationships are available:

1) a dynamical system describing the time evolution of the state variables
2) an algebraic equation that allows obtaining synchrophasor and frequency from the state variables
3) an algebraic equation mapping the states to the measurment data

Let us consider a three phase system characterized by the rated frequency f_0 (corresponding to the angular frequency ω_0). We start by choosing an expression for the measurement data (measured signal), which is the pth phase quantity ($p \in \{a, b, c\}$):

$$\begin{aligned} s_p(t) &= a_{p,1}(t)\cos\left[\omega_0 t + \varphi_{p,1}(t)\right] \\ &+ \sum_{h=2}^{M} a_{p,h}(t)\cos\left[h\omega_0 t + \varphi_{p,h}(t)\right] \end{aligned} \tag{1}$$

where $a_{p,1}(t)$ and $\varphi_{p,1}(t)$ represent the amplitude and phase angle of the phase p fundamental synchrophasor, while $a_{p,h}(t)$ and $\varphi_{p,h}(t)$ ($h \in \{2, \ldots, M\}$) denote the amplitude and phase angle of the hth harmonic synchrophasor for phase p. Of course, magnitude and phase angles are assumed as slowly varying.

Now, an expression modeling the time evolution of the synchrophasors appearing in the output equation (1) have to be introduced. For this purpose, let us consider the following quantities as state variables (time dependency is not shown explicitly for the sake of brevity):

1) the fundamental angular frequency derivatives $\omega^{(k)}$, which are supposed to be also the phase-angle derivatives of order $k+1$ for the fundamental component of each system phase, up to the order N_ω, defining the vector $\mathbf{x}_\omega$ (symbol $'\top'$ indicates the transpose operator):

$$\mathbf{x}_\omega = \begin{bmatrix} \omega^{(0)} & \omega^{(1)} & \cdots & \omega^{(N_\omega)} \end{bmatrix}^\top \tag{2}$$

2) the phase p fundamental amplitude derivatives $a_{p,1}^{(k)}$ up to the degree N_1 and its phase angle $\varphi_{p,1}$, which are the elements of $\mathbf{x}_{p,1}$:

$$\mathbf{x}_{p,1} = \begin{bmatrix} a_{p,1}^{(0)} & a_{p,1}^{(1)} & \cdots & a_{p,1}^{(N_1)} & \varphi_{p,1} \end{bmatrix}^\top \tag{3}$$

Vector $\mathbf{x}_1$ is constructed by considering all the three phases as follows:

$$\mathbf{x}_1 = \begin{bmatrix} \mathbf{x}_{a,1}^\top & \mathbf{x}_{b,1}^\top & \mathbf{x}_{c,1}^\top \end{bmatrix}^\top \tag{4}$$

3) for each generic hth harmonic, the phase p amplitude $a_{p,h}$ and phase angle $\varphi_{p,h}$, representing the components of the vector $\mathbf{x}_{p,h}$.

$$\mathbf{x}_{p,h} = \begin{bmatrix} a_{p,h} & \varphi_{p,h} \end{bmatrix}^\top \tag{5}$$

Vector $\mathbf{x}_h$ containing harmonic amplitudes and phase angles of all the phases is introduced:

$$\mathbf{x}_h = \begin{bmatrix} \mathbf{x}_{a,h}^\top & \mathbf{x}_{b,h}^\top & \mathbf{x}_{c,h}^\top \end{bmatrix}^\top \tag{6}$$

It should be noticed that a unique fundamental frequency (and its derivatives) shared by the three system phases has been considered; then, the evolutions of the harmonic phase angles for each phase p are assumed to be driven by the fundamental component. Furthermore, harmonic amplitude derivatives have not been included as state variables: since harmonics have typically much smaller magnitudes with respect to the fundamental, it is not significant to have a detailed representation of their dynamics. A noticeable reduction of the model complexity is achieved under these assumptions.

Having defined the state variables, the state vector $\mathbf{x}$ is obtained by concatenating the previously defined vectors:

$$\mathbf{x} = \begin{bmatrix} \mathbf{x}_\omega^\top & \mathbf{x}_1^\top & \mathbf{x}_2^\top & \cdots & \mathbf{x}_M^\top \end{bmatrix}^\top \tag{7}$$

It turns out that its overall length is $N = N_\omega + 1 + 3(N_1 + 2M)$.

Now, the dynamical system modeling the time evolution of the state variables has to be defined. The generic state-space expression results:

$$\frac{d\mathbf{x}}{dt} = \mathbf{A}_c \mathbf{x} \tag{8}$$

and the behavior depends on the matrix $\mathbf{A}_c$, which can be partitioned as follows:

$$\frac{d}{dt}\begin{bmatrix} \mathbf{x}_\omega \\ \mathbf{x}_1 \\ \mathbf{x}_2 \\ \vdots \\ \mathbf{x}_M \end{bmatrix} = \begin{bmatrix} \mathbf{A}_\omega & \mathbf{0} & \mathbf{0} & \cdots & \mathbf{0} \\ \mathbf{A}_{1,\omega} & \mathbf{A}_1 & \mathbf{0} & \cdots & \mathbf{0} \\ \mathbf{A}_{2,\omega} & \mathbf{0} & \mathbf{A}_2 & \cdots & \mathbf{0} \\ \vdots & \vdots & \vdots & \ddots & \mathbf{0} \\ \mathbf{A}_{M,\omega} & \mathbf{0} & \mathbf{0} & \cdots & \mathbf{A}_M \end{bmatrix} \begin{bmatrix} \mathbf{x}_\omega \\ \mathbf{x}_1 \\ \mathbf{x}_2 \\ \vdots \\ \mathbf{x}_M \end{bmatrix} \tag{9}$$

Let us define the submatrices appearing in (9); it is straightforward to obtain that $\mathbf{A}_\omega$ is a $(N_\omega + 1) \times (N_\omega + 1)$ upper shift matrix. Reminding that the evolutions of the fundamental

phase angles are assumed to be identical for the three system phases (because of the common frequency), thus $\mathbf{A}_{1,\omega}$ is a $3(N_1+2)\times(N_\omega+1)$ matrix defined as follows:

$$\mathbf{A}_{1,\omega}=\begin{bmatrix}\mathbf{0}_{(N_1+1)\times 1} & \mathbf{0}_{(N_1+1)\times N_\omega}\\ 1 & \mathbf{0}_{1\times N_\omega}\\ \mathbf{0}_{(N_1+1)\times 1} & \mathbf{0}_{(N_1+1)\times N_\omega}\\ 1 & \mathbf{0}_{1\times N_\omega}\\ \mathbf{0}_{(N_1+1)\times 1} & \mathbf{0}_{(N_1+1)\times N_\omega}\\ 1 & \mathbf{0}_{1\times N_\omega}\end{bmatrix} \tag{10}$$

Matrices $\mathbf{A}_{h,\omega}$ having size $6\times(N_\omega+1)$ are characterized by a similar structure, since the derivatives of the harmonic phase angles are supposed to be identical to that of the fundamental, but multiplied by the harmonic order h:

$$\mathbf{A}_{h,\omega}=\begin{bmatrix}0 & \mathbf{0}_{1\times N_\omega}\\ h & \mathbf{0}_{1\times N_\omega}\\ 0 & \mathbf{0}_{1\times N_\omega}\\ h & \mathbf{0}_{1\times N_\omega}\\ 0 & \mathbf{0}_{1\times N_\omega}\\ h & \mathbf{0}_{1\times N_\omega}\end{bmatrix} \tag{11}$$

Matrix $\mathbf{A_1}$ can be conveniently partitioned:

$$\mathbf{A}_1=\begin{bmatrix}\mathbf{A}_a & \mathbf{0} & \mathbf{0} & \mathbf{0} & \mathbf{0} & \mathbf{0}\\ \mathbf{0} & 0 & \mathbf{0} & 0 & \mathbf{0} & 0\\ \mathbf{0} & \mathbf{0} & \mathbf{A}_a & \mathbf{0} & \mathbf{0} & \mathbf{0}\\ \mathbf{0} & 0 & \mathbf{0} & 0 & \mathbf{0} & 0\\ \mathbf{0} & \mathbf{0} & \mathbf{0} & \mathbf{0} & \mathbf{A}_a & \mathbf{0}\\ \mathbf{0} & 0 & \mathbf{0} & 0 & \mathbf{0} & 0\end{bmatrix} \tag{12}$$

where it can be easily obtained that $\mathbf{A}_a$ is a $(N_1+1)\times(N_1+1)$ upper shift matrix. $\mathbf{A}_h$, with $h>1$, is a 2x2 null matrix.

It is useful to adopt the matrix notation also to express the three single-phase output equations (1). The vector of the three-phase measurement input $\mathbf{s}(t)$ is introduced, as well as the nonlinear time-varying vector output function $\mathbf{c}(\mathbf{x},t)$:

$$\mathbf{s}(t)=\begin{bmatrix}s_a(t)\\ s_b(t)\\ s_c(t)\end{bmatrix}=\mathbf{c}(\mathbf{x},t) \tag{13}$$

The previous equations are defined in the continuous time domain; therefore, they cannot be straightforwardly employed, since measurement data is obtained by sampling and execution is performed considering a finite time step T_s, supposed to be equal to the sampling time. The discrete time domain representation of (13) can be easily obtained by evaluating it in discrete time steps $t=kT_s$. Conversely, the continuous time state-space system (8) can be discretized obtaining the following representation:

$$\mathbf{x}(k+1)=\mathbf{A}\mathbf{x}(k) \tag{14}$$

The discretized state-space matrix $\mathbf{A}$ can be obtained from $\mathbf{A}_c$ by using the expression:

$$\mathbf{A}=e^{\mathbf{A}_c T_s} \tag{15}$$

At $t=kT_s$, (14) allows obtaining a prediction of the state $\mathbf{x}^F(k+1)$ in the next time instant $(k+1)T_s$. Matrix $\mathbf{A}$ includes blocks related to magnitudes and phase angles of both fundamental and harmonic components. Focusing, for example, on the diagonal blocks associated with the fundamental, they are upper triangular and the kth diagonal is composed by elements equal to $T_s^k/k!$ thus linking the state forecast to the truncated Taylor expansion; its order depends on the numbers of derivatives which have been considered in the continuous time representation.

Let us suppose that approximated dynamic modeling of the state variables results in equivalent zero-mean process noise having covariance matrix $\mathbf{Q}$. Under this assumption, the uncertainty of the state forecast is characterized by a covariance matrix $\mathbf{P}^F(k+1)$ given by:

$$\mathbf{P}^F(k+1)=\mathbf{A}\mathbf{P}(k)\mathbf{A}^\top+\mathbf{Q} \tag{16}$$

with $\mathbf{P}(k)$ the previous estimation covariance matrix.

Assuming that the measurement vector $\mathbf{s}$ is corrupted by zero mean noise characterized by a known covariance matrix $\mathbf{R}$, linearizing the output equation (13) with respect to the state vector $\mathbf{x}$ allows computing the minimum mean square error estimate of the state variables, which is provided by the following equation:

$$\begin{aligned}\mathbf{x}(k+1) &= \mathbf{x}^F(k+1)+\\ &+ \mathbf{K}(k+1)[\mathbf{s}-\mathbf{c}(\mathbf{x}^F(k+1),k+1)]\end{aligned} \tag{17}$$

Kalman matrix gain $\mathbf{K}(k+1)$ is obtained by computing:

$$\begin{aligned}\mathbf{K}(k+1) &= \mathbf{P}^F(k+1)\mathbf{C}^\top(k+1)\\ &\quad [\mathbf{C}(k+1)\mathbf{P}^F(k+1)\mathbf{C}^\top(k+1)+\mathbf{R}]^{-1}\end{aligned} \tag{18}$$

Where $\mathbf{C}(k+1)$ is the Jacobian of the vector function $\mathbf{c}(\mathbf{x},(k+1)T_s)$, namely:

$$\mathbf{C}(k+1)=\left.\frac{d\mathbf{c}(\mathbf{x},t)}{d\mathbf{x}}\right|_{\substack{\mathbf{x}=\mathbf{x}^F(k+1)\\ t=(k+1)T_s}} \tag{19}$$

The covariance matrix of the new estimated state is obtained as follows:

$$\mathbf{P}(k+1)=(\mathbf{I}-\mathbf{K}(k+1)\mathbf{C}(k+1))\mathbf{P}^F(k+1) \tag{20}$$

III. Obtaining Measurement and Process Noise Covariance Matrices

The behavior of the Kalman filter implementation strictly depends on the choice of the previously defined covariance matrices $\mathbf{Q}$ and $\mathbf{R}$ that define process and measurement noise, respectively. In particular, they appear in the expression (18) that allows computing the Kalman gain. Obtained estimates are as close to the optimal ones as much as these noises are able to represent measurement and model uncertainties.

Let us start with measurements, which are assumed to be affected by the errors intinsic in the measurement process, other than noise and disturbances. These effects on the three phases are supposed to be modeled by independent and identically distributed random variables. Therefore, matrix $\mathbf{R}$ can be written as:

$$\mathbf{R}=\sigma_R^2\begin{bmatrix}1 & 0 & 0\\ 0 & 1 & 0\\ 0 & 0 & 1\end{bmatrix} \tag{21}$$

Under this assumption, only the standard deviation σ_R have to be selected according to a priori knowledge.

Things becomes considerably trickier when the process noise covariance matrix $\mathbf{Q}$ has to be chosen. In this case the major uncertainty source of the state forecast is assumed to be the finite number of magnitudes and phase angle derivatives that have been included as state variables of the dynamical model. As previously stated, this results in truncated Taylor expansions of magnitudes and phase angles in the sampling instant as far as the discrete-time representation is concerned. Let us focus on the fundamental component; amplitude and phase angle modulated signals defined by the synchrophasor standard [2], [4] have been considered as representative of the typical dynamics that may occur in power systems. Their generic expression is:

$$s(t) = \sqrt{2}S[1+k_x\cos(\omega_m t)]\cos[\omega_0 t + k_a\cos(\omega_m t - \pi)] \quad (22)$$

It should be noticed that the maximum value of the kth order magnitude derivative results:

$$a_{1,max}^{(k)} = \sqrt{2}Sk_x\omega_m^k \quad (23)$$

The model includes the derivatives of the fundamental component up to the order N_1. Since $2\pi/\omega_m >> T_s$, the magnitude derivatives due to modulation can be assumed as constant during T_s. Therefore, supposing that the model starts from error-free state variables, the maximum error due only to the forecasting step of the kth order derivative can be obtained by a (N_1+1-k)-fold time integration of the maximum value of the (N_1+1)-th derivative over the sampling interval:

$$e_{a_1^{(k)}} = \sqrt{2}Sk_x\omega_m^{N_1+1}\frac{T_s^{N_1+1-k}}{(N_1+1-k)!} \quad (24)$$

Assuming a shape for the probability density function, the standard deviation $\sigma_{a_1^{(k)}}$ can be obtained from the corresponging maximum error:

$$\sigma_{a_1^{(k)}} = \frac{e_{a_1^{(k)}}}{k_c} \quad (25)$$

where k_c is a factor which is selected by assuming a confidence level for the maximum deviation.

Covariances between amplitude derivatives are obtained by assuming full correlation. On the contrary, covariances between the amplitudes of the different phases are assumed to be zero.

Identical considerations allows obtaining also the variances and covariances of the derivatives of the fundamental component phase angle (indipendently from system phase), which are assumed to be linked to angular speed derivatives.. In turns, the standard deviations of the harmonic phases can be obtained by multiplying that of the fundamental term by the harmonic order h.

In order to completely define $\mathbf{Q}$, some assumptions about the uncertainties due to the approximate modeling of harmonic amplitudes dynamics have to be introduced. A possibility is adopting a similar approach to that employed for the fundamental amplitude, hence guessing a maximum value for the first derivatives of the harmonic amplitudes which have been neglected by the model. The corresponding maximum errors during the sampling interval can be computed by integration, while the standard deviations are obtained by guessing the shape of the probability density functions. Covariances between harmonic amplitudes are assumed to be zero.

IV. Tests and Results

A. Test Assumptions

The proposed three-phase TEKF estimation algorithm has been implemented in Matlab using 1 kHz sampling rate. The following assumptions have been introduced in order to compute the covariance matrices $\mathbf{Q}$ and $\mathbf{R}$:

- Second order expansion for the fundamental amplitude and first order expansion of the angular frequency have been employed.
- Measurement noise standard deviation $\sigma_R = 3\cdot10^{-3}$ p.u. has been considered.
- Modulation angular frequency $\omega_m = 2\pi 5$ rad/s and modulation depths $k_x = 0.1$ and $k_a = 0.1$ rad for computing the maximum errors have been chosen as the most severe values reported in the synchrophasor standard.
- Maximum variation of the harmonic magnitudes within a sampling interval is assumed to be 10^{-4} p.u..
- Standard deviations have been obtained from the maximum errors by using $k_c = \sqrt{3}$.
- Harmonics up to the order $M = 9$ have been included into the model.

The performance of the estimation algorithm have been assessed under different conditions, defined by combined tests that include different excitation signals chosen among those suggested in the standard [4] and in the guide IEEE C37.242 [22]. In all the test signals, an additive white uniform noise (AWUN), at a signal-to-noise ratio (SNR) of 70 dB, is used to replicate more realistic conditions.

Positive sequence synchrophasor estimations are considered and the performance indices are the commonly adopted Total Vector Error (TVE), which indicates the relative value of the vector error magnitude, absolute frequency error (FE), along with absolute amplitude error (AE) and phase angle error (PE).

All the test scenarios in the following, except for the last one (Section IV-E) and for the AWUN contribution, are referred to balanced conditions.

B. Off-Nominal Frequency Tests

As a first test scenario, a purely sinusoidal 50 Hz signal of 1 p.u. amplitude is considered (with the aforementioned additive noise). Fig. 1 and 2 show percent TVE and frequency estimation, respectively, for a 400-ms portion of the computed quantities. The TVE is always below $0.03\,\%$ and FE < 4 mHz. Since the errors are negligible without additive noise (purely due to numerical issues), the reported results reflect the noise bandwidth of the 3ph-TEKF for the monitored quantities and the averaging properties of the Fortescue transformation that

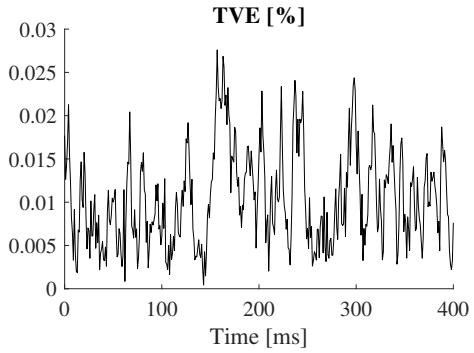

Fig. 1. TVE % under nominal conditions with 70 dB SNR.

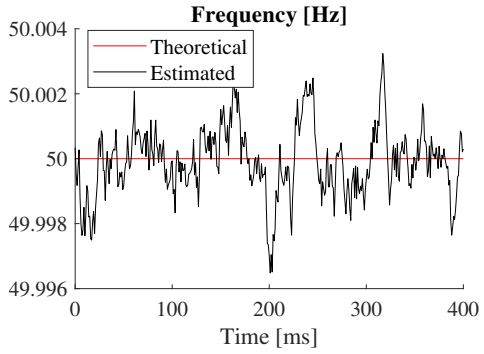

Fig. 2. FE under nominal conditions with 70 dB SNR.

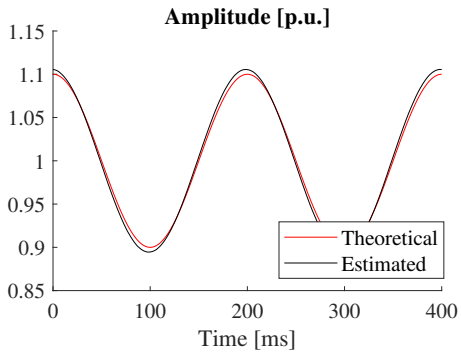

Fig. 3. Amplitude estimation in AM conditions.

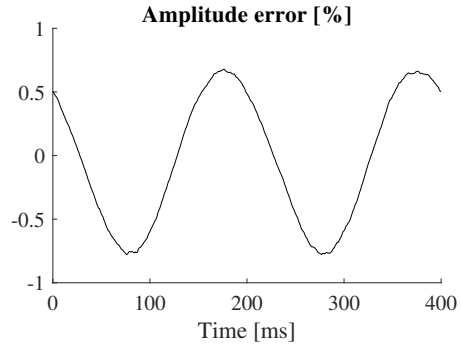

Fig. 4. Amplitude estimation in AM conditions.

has been applied to obtain the positive sequence synchrophasor.

Off-nominal frequency conditions have been simulated. Different tests have been performed considering the frequency range limits in [4]. In particular, the tests with $f = 45\,\text{Hz}$ and $f = 55\,\text{Hz}$ confirm the frequency tracking capability of the filter. Errors are almost the same as those obtained under nominal frequency, thus confirming that the main contribution comes from noise.

C. Harmonic Disturbance Tests

A second set of tests has been performed by adding three harmonics to the fundamental component. In particular, harmonic orders 3, 5, and 7 have been considered (among the most relevant in real-world scenarios). Magnitude is $5\,\%$ of the fundamental for all the harmonic orders (random initial phase angles are considered) and tests at nominal and off-nominal frequencies (49 and $51\,\text{Hz}$) have been performed. The 3ph-TEKF shows remarkable harmonic rejection: the worst case occurs when $f = 51\,\text{Hz}$ with an average TVE $= 0.0789\,\%$[1].

It is important to highlight that, as in the previous tests, errors becomes negligible once additive noise is removed, thus confirming that harmonics can be easily ruled out when the employed model includes them.

[1]the last 400 ms of a 10s simulation are considered and shown with relative timescale.

D. Modulation Tests

Since the focus of the proposed method is on dynamic conditions, modulation tests have been considered as representative of time-varying test signals. In particular, sinusoidal amplitude and phase-angle modulations are adopted (referred to as AM and PM in the following), using the signal in (22). Frequency modulation $f_m \in (0, 5]\,\text{Hz}$ with modulation indices $k_x = 0.1$ and $k_a = 0.1\,\text{rad}$, respectively for AM and PM, is used. In the following, results for $f_m = 5\,\text{Hz}$ in the AM test case are discussed. Fig. 3 and Fig. 4 show the synchrophasor amplitude estimation and the corresponding AE. Since PE values are below $0.03\,\text{crad}$, TVE is mainly influenced by AE (maximum value $0.78\,\%$).

FE values are almost unaffected by the changing amplitude and the results are similar to those obtained under steady-state conditions.

PM modulation ($f_m = 5\,\text{Hz}$) leads to negligible AEs (with respect to additive noise contribution) while PE and FE values become higher. Fig. 5 shows the TVE evolution, which directly reflects the PE behaviour. FEs are reported in Fig. 6 and are below $140\,\text{mHz}$. The oscillatory behaviour of the error is strictly related to the approximate modeling of phase-angle dynamics, which is not able to consider all its derivatives.

E. Unbalance Tests

Three-phase systems and, in particular, distribution systems may suffer from a certain level of unbalance between phases. For this reason, [22] suggests to test instrumentation under the

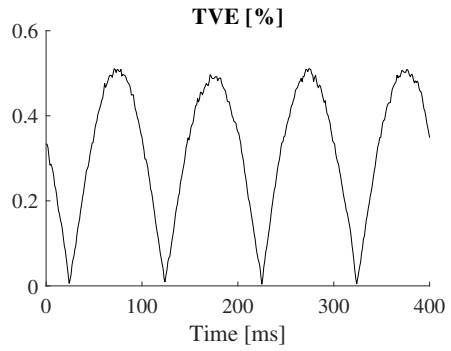

Fig. 5. TVE % in PM conditions.

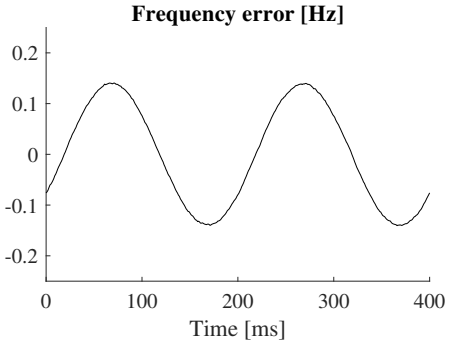

Fig. 6. FE in PM conditions.

following imbalances: magnitude $\pm 10\,\%$, and $\pm 20\,\%$ on one phase only; phase $\pm 60°$, $\pm 40°$, and $\pm 20°$ on one phase only. Unbalance should be applied to both $f = 50$ and $49\,\mathrm{Hz}$. In all the performed tests, the effect of amplitude unbalance is negligible with respect to the contribution due to additive noise because all the three-phase magnitudes are included in the state vector (7). Phase-angle unbalance corresponds instead to a different initial condition for the three phase angles and thus, after a transient, the 3ph-TEKF is able to accurately perform the measurements. A disturbance appears in the frequency estimate, but its amplitude is almost completely masked by the effect of noise.

V. Conclusions

Synchrophasor and frequency measurement algorithms based on Kalman filtering have become popular in the last years. The main advantage is achieving very low latency, which is an important feature for time-critical applications. In this work, a full three-phase Extended Kalman Filter synchrophasor estimator is proposed for the first time. The introduced simplifications allows reducing the computational cost, while obtaining remarkable dynamic performance and good rejection of disturbances and unbalance. In addition, the proposed implementation also permits estimating harmonic components, which represents an important feature when it is employed in distribution grids.

Acknowledgements

Dr. Pegoraro work was partially funded by Fondazione di Sardegna for the research project "SUM2GRIDS, Solutions by mUltidisciplinary approach for intelligent Monitoring and Management of power distribution GRIDS".

References

[1] AA. VV., *Phasor Measurement Units and Wide Area Monitoring Systems*, 1st ed., A. Monti, C. Muscas, and F. Ponci, Eds. Academic Press, 2016.

[2] *IEEE Standard for Synchrophasor Measurements for Power Systems*, IEEE Std C37.118.1-2011, Dec. 2011.

[3] *IEEE Standard for Synchrophasor Measurements for Power Systems – Amendment 1: Modification of Selected Performance Requirements*, IEEE Std C37.118.1a-2014, Apr. 2014.

[4] *IEEE/IEC International Standard - Measuring relays and protection equipment - Part 118-1: Synchrophasor for power systems - Measurements*, IEEE/IEC IEC/IEEE 60255-118-1:2018, Dec 2018.

[5] J. A. de la O Serna, "Dynamic phasor estimates for power system oscillations," *IEEE Trans. Instrum. Meas.*, vol. 56, no. 5, pp. 1648–1657, Oct. 2007.

[6] W. Premerlani, B. Kasztenny, and M. Adamiak, "Development and implementation of a synchrophasor estimator capable of measurements under dynamic conditions," *IEEE Trans. Power Del.*, vol. 23, no. 1, pp. 109–123, Jan. 2008.

[7] R. K. Mai, Z. Y. He, L. Fu, B. Kirby, and Z. Q. Bo, "A dynamic synchrophasor estimation algorithm for online application," *IEEE Trans. Power Del.*, vol. 25, no. 2, pp. 570–578, Apr. 2010.

[8] G. Frigo, A. Derviskadic, and M. Paolone, "Reduced leakage synchrophasor estimation: Hilbert transform plus interpolated dft," *IEEE Trans. Instrum. Meas.*, pp. 1–16, 2018.

[9] D. Petri, D. Fontanelli, and D. Macii, "A frequency-domain algorithm for dynamic synchrophasor and frequency estimation," *IEEE Trans. Instrum. Meas.*, vol. 63, no. 10, pp. 2330–2340, Oct. 2014.

[10] P. Castello, J. Liu, C. Muscas, P. A. Pegoraro, F. Ponci, and A. Monti, "A fast and accurate PMU algorithm for P+M class measurement of synchrophasor and frequency," *IEEE Trans. Instrum. Meas.*, vol. 63, no. 12, pp. 2837–2845, Dec. 2014.

[11] S. Toscani and C. Muscas, "A space vector based approach for synchrophasor measurement," in *IEEE I2MTC*, May 2014, pp. 257–261.

[12] P. Castello, R. Ferrero, P. A. Pegoraro, and S. Toscani, "Space vector taylor-fourier models for synchrophasor, frequency, and rocof measurements in three-phase systems," *IEEE Trans. Instrum. Meas.*, vol. 68, no. 5, pp. 1313–1321, May 2019.

[13] M. Bertocco, G. Frigo, C. Narduzzi, C. Muscas, and P. A. Pegoraro, "Compressive sensing of a taylor-fourier multifrequency model for synchrophasor estimation," *IEEE Trans. Instrum. Meas.*, vol. 64, no. 12, pp. 3274–3283, Dec 2015.

[14] I. Kamwa, S. R. Samantaray, and G. Joos, "Wide frequency range adaptive phasor and frequency pmu algorithms," *IEEE Trans. Smart Grid*, vol. 5, no. 2, pp. 569–579, Mar. 2014.

[15] J. A. de la O Serna and J. Rodriguez-Maldonado, "Instantaneous oscillating phasor estimates with taylor-kalman filters," *IEEE Trans. Power Syst.*, vol. 26, no. 4, pp. 2336–2344, Nov. 2011.

[16] J. Liu, F. Ni, J. Tang, F. Ponci, and A. Monti, "A modified Taylor-Kalman filter for instantaneous dynamic phasor estimation," in *IEEE PES Innovative Smart Grid Technologies (ISGT) Eur. Conf.*, 2012.

[17] D. Fontanelli, D. Macii, and D. Petri, "Dynamic synchrophasor estimation using smoothed kalman filtering," in *IEEE I2MTC*, May 2016.

[18] J. de la O Serna and J. Rodriandguez-Maldonado, "Taylor-Kalman-Fourier filters for instantaneous oscillating phasor and harmonic estimates," *IEEE Trans. Instrum. Meas.*, vol. 61, no. 4, pp. 941–951, Apr. 2012.

[19] J. Liu, F. Ni, P. A. Pegoraro, F. Ponci, A. Monti, and C. Muscas, "Fundamental and harmonic synchrophasors estimation using modified taylor-kaiman filter," in *Proc. of IEEE AMPS*, Sep. 2012, pp. 1–6.

[20] R. Ferrero, P. A. Pegoraro, and S. Toscani, "Dynamic fundamental and harmonic synchrophasor estimation by extended kalman filter," in *Proc. of IEEE Appl. Meas. for Pow. Syst. (AMPS)*, Sep. 2016, pp. 1–6.

[21] S. Toscani, C. Muscas, and P. A. Pegoraro, "Design and performance prediction of space vector-based pmu algorithms," *IEEE Trans. Instrum. Meas.*, vol. 66, no. 3, pp. 394–404, Mar. 2017.

[22] *IEEE Guide for Synchronization, Calibration, Testing, and Installation of PMUs for Power System Protection and Control*, IEEE C37.242-2013, Mar. 2013.

[23] P. Castello, R. Ferrero, P. A. Pegoraro, and S. Toscani, "Effect of unbalance on positive-sequence synchrophasor, frequency, and rocof estimations," *IEEE Trans. Instrum. Meas.*, vol. 67, no. 5, pp. 1036–1046, May 2018.